TECHNICAL UNIVERSITY OF CLUJ-NAPOCA

ACTA TECHNICA NAPOCENSIS

Series: Applied Mathematics, Mechanics, and Engineering
Vol. 69, Issue Special I, February, 2026

MICRO-GEOMETRIC STRUCTURAL ANALYSIS OF FDM 3D PRINTED PARTS USING COMPUTER TOMOGRAPH IMAGING

Vlad-Cristian ENACHE, George VLĂSCEANU, Mihaela-Elena ULMEANU, Cristian-Vasile DOICIN, Nicolae IONESCU

Abstract: *This paper presents a structural and micro-geometric analysis of Fused Deposition Modeling 3D printed parts using Computed Tomography imaging as a non-destructive evaluation tool. Samples were fabricated using a Prusa MK4S, with key parameters such as wall line count, wall thickness, and infill density, systematically varied. The 3D geometry and internal structure of the printed parts were scanned using an industrial CT system, a Bruker SkyScan 1272. Based on the CT results, the actual density of each sample was calculated and compared with the values provided by the manufacturer. An ANOVA statistical analysis was performed to evaluate the influence of the FDM parameters that were previously varied on the measured density variability. Additionally, qualitative inspection of the CT data enabled identification of characteristic manufacturing defects, including deformations on the interface between rectangular and cylindrical surfaces, weak layer adhesion between macro-volumes, and filament detachment at sharp toolpath transitions (≥45°). These findings provide critical insights into the microstructural fidelity of FDM processes and support future optimization strategies for additive manufacturing reliability.*

Key words: *Computed Tomography, Additive Manufacturing Defects, Micro-geometric Analysis, Density Evaluation.*

1. INTRODUCTION

Additive Manufacturing (AM) is now a well-known production set of processes in which three-dimensional objects are constructed by sequentially adding material, layer by layer, based on a digital model. In contrast to traditional manufacturing methods that typically involve removing or shaping material, AM enables the direct fabrication of complex geometries with greater design flexibility and reduced material waste.

AM technologies have the advantage of allowing its users to create parts with fewer components that otherwise would be impossible to make with subtractive manufacturing processes [1]. Fused Deposition Modelling (FDM) is one of the most commonly used AM technologies due to its' high accessibility, open-source support platforms, low costs (software, machine and materials) and versatility of the applications. The FDM process is quite simple, a thermoplastic material is melted and then deposited layer by layer. The machine deposits each layer according to the CAD model that was previously created and processed through its specific slicer software. In the slicer software, the user has the freedom to change each of the printing parameters according to its needs, to the part mechanical use and to the material capabilities of usage [2].

Like all technologies, FDM has some disadvantages and limitations. Some of the most common are the presence of voids and inclusions due to the lack of material or recrystallization, mechanical anisotropy as a consequence of layer-by-layer building, reduced resistance against external forces, surface inconsistencies and residual stress caused when the material heating is uneven [3].

Another disadvantage to FDM 3D printed parts is that after fabrication, most of the parts are thin walled, their walls having the width of the extruded fiber. It is almost impossible to create walls thinner than 1 mm, or the walls are very brittle due to this cause. The surface finish

always depends on the layer height and build angle [4]. These constructive limitations are intrinsic to FDM, correlated to the capabilities of the machine, the type of material and other used resources.

In an effort to study the possibility of improving these limitations, this paper proposes to analyze micro-geometric changes that occur in the internal structure of the 3D printed samples using Computer tomography (CT) scanning and parameter influence on the density of FDM 3D printed samples.

CT scanning is a non-destructive assessment technique for 3D printed parts that is widely used, compared to other conventional tests that might destroy the parts in the process, or their structure [5]. CT as a non-destructive technique can offer three-dimensional evaluation of internal defects, being highly beneficial and favorable to determine internal defects and cavities. It is also widely used to determine the porosity, density, dimensional analysis and surface roughness of the studied parts. For the current experimental evaluation, the specimen was subjected to scanning from three different points by rotating it through angular increments. The final image was reconstructed using specific software and further analyzed [6].

2. METHODS AND MATERIALS

This study involved the analysis of 24 samples fabricated through FDM using polylactic acid (PLA) filament. All specimens were produced with the same PLA material (Winkle PLA) sourced from a single manufacturer, but in two distinct color variants: black and white. The choice of color was intended to evaluate whether pigment composition influences the material's density and, consequently, the overall weight of the printed parts.

The selected sample geometry (Figure 1) was intentionally designed to combine both rectangular and cylindrical volumes in a single part. This configuration allows for the simultaneous investigation of macro-geometric features, such as how dissimilar shapes merge within a single print, as well as micro-geometric characteristics, including surface texture and layer adhesion on curved versus flat regions. The junction between the two volumes is particularly relevant for analyzing dimensional accuracy and material behavior at complex interfaces in FDM printing.

Sample fabrication was carried out on a Prusa MK4S 3D printer, and the technical specifications of the equipment are detailed in Table 1.

Table 1

Prusa MK4S characteristics [7]

Measurements	
Build Volume	250x210x220 mm
Filament diameter	1.75 mm
Layer height	0.05-0.30 mm
Printer dimensions	7 kg, 500x550x400 mm
Extruder	
Extruder	Nextruder, Direct Drive, E3D V6 compatible
Filament path	Aluminum heatsink
Nozzle	0.4 mm
Maximum operating temperature	
Max nozzle temperature	290°C
Max heatbed temperature	120°C
Print surface	
Print surface	Magnetic heatbed with removable PEI spring steel sheets
Materials	
Supported materials	PLA, PETG, Flex, PVA, PC, PP, CPE, PVB
Power	
PSU	240W
Power consumption	PLA settings: 80W/ABS settings: 120W

All samples were individually fabricated on the 3D printer's build plate, maintaining a consistent orientation as shown in Figure 1. To evaluate the influence of printing parameters on both the micro-geometry and material density of the parts, three slicer settings were systematically varied: wall line count, infill percentage, and default layer thickness. These parameters were selected due to their known impact on internal structure, surface quality, and overall material distribution in FDM-printed components [3].

Understanding how these variables interact is essential for optimizing mechanical performance and dimensional accuracy in functional 3D printed parts.

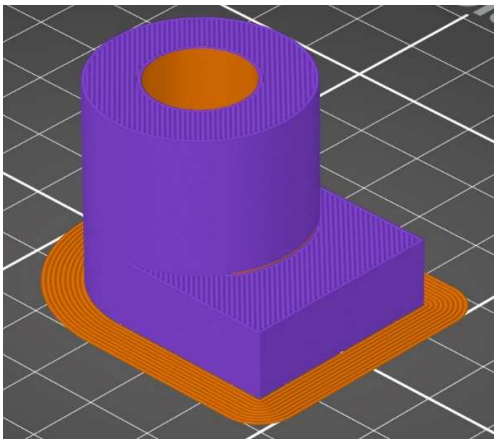

Fig. 1. The sample position in PrusaSlicer

The experimental design was structured around a Taguchi L12 orthogonal array, which enabled the exploration of multiple parameter combinations while minimizing the total number of required experiments. The three selected process parameters were each assigned three discrete levels (minimum, average, and maximum) to ensure a representative sampling across their respective ranges. The specific values for each level are provided in Table 2. This approach supports a statistically robust evaluation of the influence of printing parameters on the material density and micro-geometric characteristics of the fabricated samples.

Table 2

The levels for each parameter

No.	Parameter	Minimum	Average	Maximum
1	Infill	15%	40%	100%
2	Wall Line Count	1	2	3
3	Default Thickness	0,45 mm	0,67 mm	1 mm

The usage of a Taguchi L12 orthogonal array ensured efficient coverage of the parameter space while minimizing experimental effort and reducing potential error. This design also enhances the reliability of subsequent statistical evaluations, such as ANOVA. To improve the robustness of the analysis, the intermediate (average) levels of each parameter were replicated four times. The complete distribution of experimental conditions is detailed in Table 3.

In addition to the three variable parameters, all other printing settings were held constant to ensure experimental consistency.

Table 3

L12 Taguchi matrix -white and black samples

Sample No.	Variables		
	Infill	Wall Line Count	Default Thickness
E1	40%	2	0,67 mm
E2	15%	1	0,45 mm
E3	15%	1	1 mm
E4	15%	3	0,45 mm
E5	15%	3	1 mm
E6	40%	2	0,67 mm
E7	100%	3	1 mm
E8	100%	3	0,45 mm
E9	100%	1	1 mm
E10	100%	1	0,45 mm
E11	40%	2	0,67 mm
E12	40%	2	0,67 mm

A fixed printing speed of 50 mm/s was used across all samples. To improve adhesion to the build plate, a 6 mm brim was added to each print. Two sets of 12 samples were produced using the same PLA material from the Winkle brand, in two different color variants: HD White and Jet-Black. All prints were carried out under identical environmental conditions and ambient temperature, without the use of an enclosed printer. The full set of printing parameters applied throughout the study is summarized in Table 4. This controlled setup helped isolate variable effects and reduce external influences.

Table 4

3D printing settings

Layer Height	0.2 mm
First Layer Height	0.2 mm
Perimeters	(1 .. 3)
Fill Pattern	Rectilinear
Brim Type	Outer brim only
Brim Width	6 mm
Perimeters	50 mm/s
Small perimeters	50 mm/s
External perimeters	50 mm/s
Infill	50 mm/s
Solid infill	50 mm/s
Top solid infill	50 mm/s
Support material	50 mm/s
Gap fill	50 mm/s
Default extrusion width	(0.45 .. 1) mm
Infill	(15 .. 100) %

Following the 3D printing process, all samples were subjected to computer tomography scanning to gain a deeper understanding of their internal structure and to accurately determine their material density. These results were then compared to the reference density values provided in the manufacturer's technical data sheet [8].

To ensure comprehensive analysis, each sample was scanned at three distinct locations, allowing for spatial variation in internal features to be captured and visualized through high-resolution 3D reconstructions. Prior to scanning, the ambient temperature of the CT environment was monitored and maintained within an optimal range to ensure imaging consistency and minimize thermal artifacts.

The CT scanner that was used is a SKYSCAN 1272 CMOS Edition, which is a high-resolution 3D X-ray Microscope. The main technical characteristics of this CT scanner are presented in Table 5.

Table 5

SKYSCAN 1272 CMOS characteristics [9]

X-ray source	40 – 100 kV
	10 W
	<5 µm spot size at 4 W
X-ray detector	16 MP sCMOS detector
Object size	75 mm diameter
	80 mm height
Sample changer	16 samples up to 25 mm diameter
Dimensions	1160 mm x 520 mm x 330 mm
Power supply	100-240V AC, 50-60 Hz

3. RESULTS

The initial stage of the analysis involved comparing the measured density of each sample with the reference density values provided by the manufacturer for the PLA material.

According to the technical specifications [8], both the white and black PLA material options from Winkle share identical material properties, as detailed in Table 6.

The density of each of the 24 printed samples was determined by combining mass and volume measurements. Prior to scanning, all samples were weighed using a high-precision Pioneer Plus PA323 electronic scale to ensure accurate mass measurements with four-digit accuracy.

Table 6

Material characteristics for White PLAWinkle and Black PLA Winkle [8]

Density	1.24 g/cm^3
Flow Rate(210°C/2.16KG)	8 g/10 min
Flow Rate(190°C/2.16KG)	3 g/10 min
Melting temperature	155°C
Glass transition temperature	55°C - 60°C
Nozzle temperature	190°C-230°C
Hot bed temperature	50°C-70°C
Cooling Fan	ON

The volume of each part was then extracted from the 3D reconstruction data obtained through micro-computed tomography (CT) scanning. Using these two variables, the density of each individual sample was calculated using the standard formula: density = mass / volume. The calculated densities for both the white and black PLA samples were then compared against the reference value provided by the manufacturer. As presented in Table 7 for the white PLA and Table 8 for the black PLA, notable deviations were observed between the experimental and nominal density values. In all cases, the measured densities were consistently lower than the value specified in the material datasheet, indicating potential variations in material deposition or internal porosity introduced during the printing process. These variations highlight the need to optimize process parameters for reliable material performance targeting different functional applications.

Table 7

Density for white samples

Sample No.	Density [g/cm^3]	Winkle PLA density[g/cm^3]	Difference
E1_A	1.0964	1.24 [8]	0.14
E2_A	0.9380		0.05
E3_A	0.9889		0.3
E4_A	0.9979		0.29
E5_A	1.1316		0.25
E6_A	0.9881		0.22
E7_A	1.2132		0.24
E8_A	1.2500		0.25
E9_A	1.2016		0.11
E10_A	1.1305		0.05

E11_A	1.1528		0.29
E12_A	1.1661		0.23

Table 8

Density for black samples

Sample No.	Density [g/cm^3]	Winkle PLA density[g/cm^3]	Difference
E1_N	1.1919	1.24 [8]	0.05
E2_N	0.9380		0.30
E3_N	0.9526		0.29
E4_N	0.9889		0.25
E5_N	1.0186		0.22
E6_N	0.9979		0.24
E7_N	0.9903		0.25
E8_N	1.1316		0.11
E9_N	1.1888		0.05
E10_N	0.9881		0.25
E11_N	1.0128		0.23
E12_N	1.2132		0.03

To provide a clearer interpretation of the data and assess the consistency within each group of samples, the average density and standard deviation were calculated for each set of samples, as presented in Table 9.

Table 9

Average and standard deviation values

Sample color	Average [g/cm^3]	Standard deviation [g/cm^3]	Differences from PLA
White	1.1046	0.1027	-0.1354
Black	1.1412	0.1134	-0.0988

The calculated density values indicate that both the white and black PLA samples show lower densities compared to the reference values. This discrepancy may be attributed to the presence of internal voids, pigment-induced variations in material behavior, or inconsistencies in the printing process. Notably, the black PLA samples show densities closer to the nominal value, suggesting a potentially more compact internal structure. While the white PLA appears to have a more uniform material distribution, the black PLA demonstrates better performance in terms of overall density. Following the density analysis, a graphical evaluation of wall thickness distribution was conducted to further investigate geometric uniformity (Figure 2).

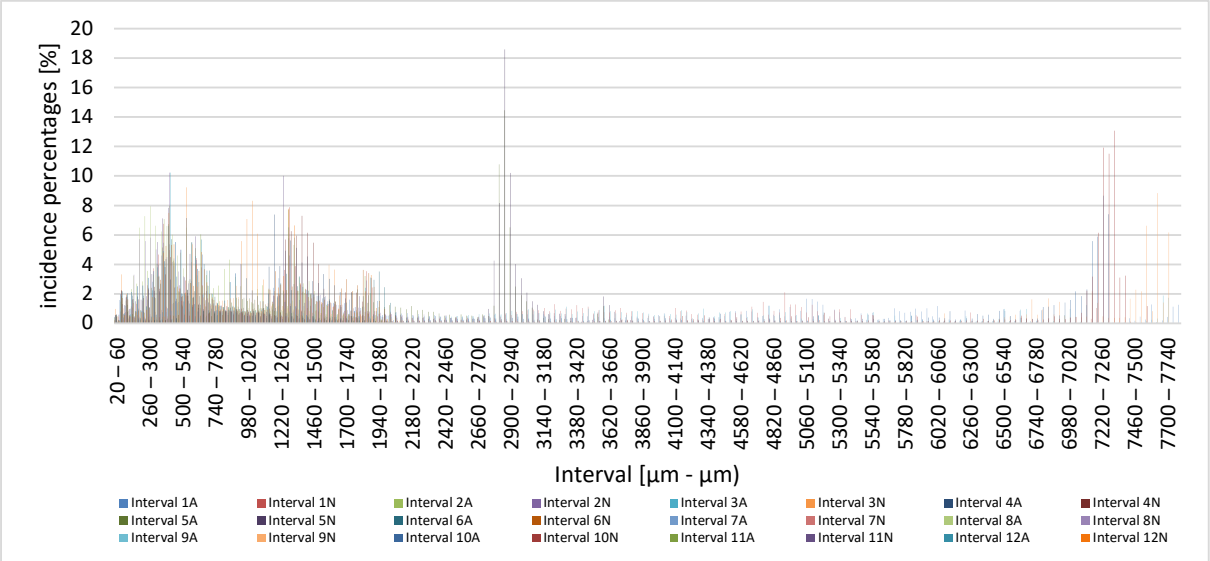

Fig. 2. Wall width distribution for all the 24 samples

An analysis of the wall thickness distribution reveals that the majority of the measured values fall within the range of 220 µm to 1660 µm. This distribution indicates that most of the sample walls fall within a relatively thin range, between approximately 0.2 mm and 1.6 mm. Notably, samples 4, 9, and 12 show localized increases in wall thickness within this interval, deviating from the general trend. These observations suggest that wall thickness is not uniformly distributed across all samples, highlighting potential inconsistencies in the printing process. Further investigation is required to determine the underlying causes of these variations and their potential impact on part performance and structural integrity.

3.1. The influence of infill, wall line count and default thickness on density

In order to determine the influence of infill, wall line count and default thickness parameters influence on the density of the samples, a ANOVA analysis was performed. ANOVA, or Analysis of Variance, is based on the independent variable, which in this case is density, and three data sets for infill, wall line count and default thickness for each of the 24 samples. Because each factor has multiple levels and the experiment is following a L12 Taguchi design, ANOVA is an ideal tool to determine whether the variations of these parameters influence the change in density. In this way, it can be determined in what way each parameter contributes to the desired result. The values for each parameter from the ANOVA analysis are presented in Table 10.

Table 10

ANOVA results for the three studied parameters: infill, wall line count and default thickness

White samples			
	F-stat	**P-value**	**Interpretation**
Infill	6.4484	0.0183	Significant
Wall line count	0.6178	0.5605	Not significant
Default thickness	0.2484	0.7851	Not significant
Black samples			
	F-stat	**P-value**	**Interpretation**
Infill	6.3341	0.0191	Significant
Wall line count	0.2346	0.7955	Not significant
Default thickness	0.5668	0.5863	Not significant

By analyzing the ANOVA results, the only factor that showed a significant influence ($p < 0.05$) is the *Infill* parameter showing that the print density is strongly influenced by the infill density of each part. On the other hand, wall line count and default thickness do not affect the results in any way.

3.2. Visual analysis from CT of the samples

An examination of the CT scan images reveals several structural imperfections and surface anomalies, which are highlighted in Figures 3, 4, and 5. Out of the 24 samples three were selected for visual representation of the encountered flaws, one with 15% infill and 1 outer wall, one with 40% infill and 2 outer walls and one sample with 100% infill. Upon analyzing the CT scan data for samples printed with 15% and 40% infill, localized printing anomalies were observed. In specific regions, the 3D printer appears to have deviated from its intended toolpath, particularly in areas requiring a 45° directional change. Instead of forming the expected angular transitions, the material deposition exhibits a slight curvature, resulting in circular surface features. This irregularity is not uniform across the entire sample but is confined to distinct zones. The described phenomenon is illustrated for sample E1_A in Figure 3.a and for sample E4_N in Figure 4.a.

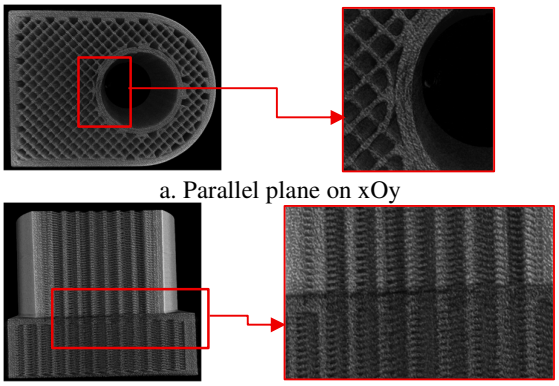

a. Parallel plane on xOy

b. Parallel plane on xOz

Fig. 3. Sample E1_A interior structure

Another noticeable flaw, observed consistently across all 24 samples, is the presence of an internal contrast (or layer dislodgement) at the interface between macro-geometric elements, specifically, in regions where different geometric shapes converge (Figures 3b, 4b and 5b). This contrast appears as a subtle but distinct variation in material density or structure within the interior of the part. In some cases, a similar pattern is faintly visible on the external surfaces as well, suggesting that the transition between geometries may influence both internal continuity and external finish. This defect may be attributed to factors such as Z-axis calibration issues, extrusion inconsistencies, or suboptimal thermal conditions during printing, such as incorrect nozzle temperature or improper fan speed. However, additional testing is required to validate these hypotheses and identify the exact cause.

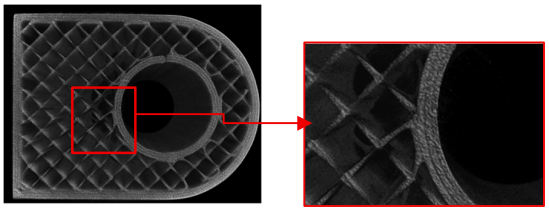

a. Parallel plane on xOy

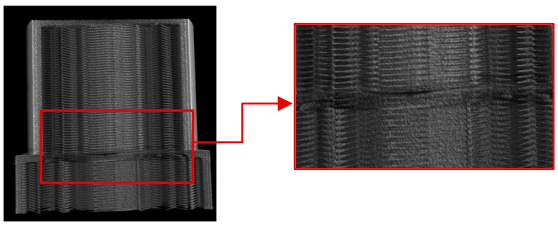

b. Parallel plane on xOz

Fig. 4. Sample E4_N interior structure

Another defect, better observed in the samples with 100% infill, is the incomplete fusion between the infill structure and the outer perimeter walls (Figure 5.a). Despite being designed as nearly solid parts, these samples exhibit internal voids near the boundary regions.

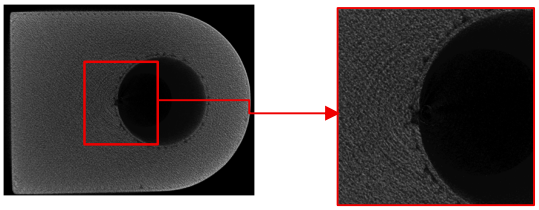

a. Parallel plane on xOy

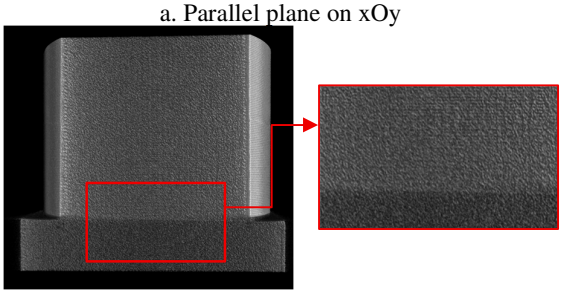

b. Parallel plane on xOz

Fig. 5. Sample E10_A interior structure

This issue may be related to variations in flow rate or extrusion width during the printing process, potentially affecting the bonding between adjacent material paths. T

The contrast at the interface between different macro-geometric features is more distinct in the fully filled samples, likely due to the increased material density and reduced internal porosity.

4. CONCLUSION

This paper studied the microstructural geometry of 3D printed samples using CT imaging. 24 samples were printed using a Prusa MK4S, with two different colors of PLA from the same manufacturer. The samples had three printing parameters varied: infill density, wall line count and the default thickness of the melted filament. The parts had their density calculated using a CT machine, a SkyScan 1272 CMOS, and compared with the density that was recommended by the manufacturer. The parts had slightly different densities than the one that was recommended of 1.24 g/cm^3. Their density varied below this threshold. This can be caused by multiple factors, such as the material pigment, the FDM machine's printing temperature threshold, but further tests are needed in order to confirm this. Also from the CT scans, the distribution of wall thickness was presented, which showed that many of the samples had a thickness between 0.2 mm and 1.66 mm, with some specific samples that were outside this range. Visual analysis of the CT images showed certain defects that appeared in their inner structures. As presented, all the samples presented the same defects, which was a slight deviation of the printing machine when it printed the infill structure. At certain angles in the inner structure, when the nozzle should create a 45°angle that is related to the outer wall, the nozzle would go instead in an almost circular motion as presented. Another defect that was visible was a contrast between the macro-geometric structures, when the different shapes of the samples were merged. For future research, the authors proposed a study of the positions of the samples on the FDM machine printing bed, in order to see if it also affects the internal structure. Also, further tests for the fan speed are needed to check if it also influences the internal structure.

5. REFERENCES

[1] **Guo, N., Leu, M.C.** *Additive manufacturing: Technology, applications and research needs*, Frontiers of Mechanical Engineering in China, ISSN: 2095-0233, China, 2013.

[2] **Common FDM 3D Printing Defects**, International Congress on 3D Printing (Additive Manufacturing) Technologies and Digital Industry, April 2018.
[3] **Bahnini, I., Rivette, M., Rechia, A., Siadat, A., Elmesbahi, A.** *Additive manufacturing technology: The status, applications, and prospects*, International Journal of Advanced Manufacturing Technology, ISSN: 0268-3768, UK, 2018.
[4] **Gajdoš, I., Slota, J.** *Influence of Printing Conditions on Structure in FDM Prototypes***,** Technical Gazette, ISSN 1330-3651, Vol. 20, No. 2, pp. 231–236, Croatia, 2013.
[5] **Taheri, H., Koester, L., Bigelow, T., Bond, L. J.,** *Finite Element Simulation and Experimental Verification of Ultrasonic Non-Destructive Inspection of Defect in Additively Manufactured Materials*, Proceedings of the 44th Annual Review of Progress in Quantitative Nondestructive Evaluation, Provo, Utah, USA, Editors Dale E. Chimenti and Leonard J. Bond, vol. 1949, Issue 1, 2018, pp. 020011-1 - 020011-13, ISBN: 978-0-7354-1644-4
[6] **Khosravani, M. R., Reinicke, T.** *On the Use of X-ray Computed Tomography in Assessment of 3D-Printed Components*
[7] Original Prusa MK4S 3D Printer, https://www.prusa3d.com/product/original-prusa-mk4s-3d-printer-5/
[8] Material characteristics and data sheet, https://winkle.shop/producto/filamento-pla-mate-winkle-175-mm-1-kg-blanco-nata/
[9] 3D X-ray Microscopy (XRM), SKYSCAN 1272 CMOS Edition, https://www.bruker.com/en/products-and-solutions/diffractometers-and-x-ray-microscopes/3d-x-ray-microscopes/skyscan-1272.html

Analiza Structurală Microgeometrică a Pieselor Imprimate 3D - FDM utilizând Imagistica Tomografică Computerizată

Această lucrare prezintă o analiză structurală și micro-geometrică a pieselor imprimate 3D prin tehnologia FDM, utilizând tomografia computerizată ca metodă de evaluare nedistructivă. Probele au fost fabricate cu ajutorul unei imprimante FDM Prusa MK4S, variind sistematic anumiți parametri esențiali precum numărul de perimetre, grosimea peretelui și densitatea umplerii. Geometria 3D și structura internă a pieselor imprimate au fost scanate utilizând un sistem industrial de tomografie computerizată, Bruker SkyScan 1272. Pe baza rezultatelor CT, densitatea reală a fiecărui eșantion a fost calculată și comparată cu valorile specificate de producător. A fost realizată o analiză statistică de tip ANOVA pentru a evalua influența parametrilor FDM variați asupra variabilității densității măsurate. În plus, inspecția calitativă a datelor CT a permis identificarea unor defecte caracteristice ale procesului de fabricație, precum deformări la interfața dintre suprafețe cilindrice și dreptunghiulare, aderență slabă între straturi în zonele de macro-volume și desprinderi de filament în zonele de tranziție bruscă a traiectoriei de extrudare (≥45°). Aceste constatări oferă perspective esențiale asupra fidelității microstructurale a procesului FDM și susțin strategiile viitoare de optimizare a fiabilității în fabricația aditivă.

Vlad Cristian ENACHE, PhD. Student, Assistant, National University of Science and Technology POLITEHNICA Bucharest, Faculty of Industrial Engineering and Robotics, Department of Manufacturing, vlad.enache1103@upb.ro, Splaiul Independenței 313, Bucharest 060042.
George VLĂSCEANU, Assistant, National University of Science and Technology POLITEHNICA Bucharest, Faculty of Medical Engineering, george.vlasceanu@upb.ro, Splaiul Independenței 313, București 060042; Academy of Romanian Scientists, Ilfov 3, 050044 Bucharest, Romania.
Mihaela-Elena ULMEANU, corresponding author, PhD. Eng., Assoc. prof., National University of Science and Technology POLITEHNICA Bucharest, Faculty of Industrial Engineering and Robotics, Department of Manufacturing, mihaela.ulmeanu@upb.ro, Splaiul Independenței 313, București 060042; Academy of Romanian Scientists, Ilfov 3, 050044 Bucharest, Romania, +40 766 289 886.
Cristian-Vasile DOICIN, PhD. Eng., Professor, National University of Science and Technology POLITEHNICA Bucharest, Faculty of Industrial Engineering and Robotics, Department of Manufacturing, cristian.doicin@upb.ro, Splaiul Independenței 313, Bucharest 060042.
Nicolae IONESCU, PhD. Eng., Professor, National University of Science and Technology POLITEHNICA Bucharest, Faculty of Industrial Engineering and Robotics, Department of Manufacturing, nicolae.ionescu@upb.ro, Splaiul Independenței 313, Bucharest 060042.